

Assessment of Regional Myocardial Motion in Dystrophin-Deficient *mdx* Mice Revealed Biphasic Functional Adaptations

W. Liu^{1,2}, J. Chen^{1,2}, J. S. Allen¹, R. M. Grady³, S. A. Wickline^{1,2}, X. Yu^{1,2}

¹Cardiovascular MR Laboratories, Washington University School of Medicine, St. Louis, MO, United States, ²Department of Biomedical Engineering, Washington University, St. Louis, MO, United States, ³Department of Pediatrics, Washington University School of Medicine, St. Louis, MO, United States

Introduction

The dystrophin-glycoprotein complex (DGC) maintains the structural integrity of the muscle fibers by linking the intracellular cytoskeleton to the overlying basal lamina. Of critical importance is the well-characterized cytoplasmic protein, dystrophin. Dystrophin mediates structural functions, by binding to cytoskeleton actin, as well as signaling functions, by binding to α -dystrobrevin and syntrophin, which anchor signaling molecules such as neuronal nitric oxide synthase. The *mdx* mouse, a model of Duchenne muscular dystrophy, carries a nonsense mutation in the dystrophin gene that eliminates the expression of dystrophin. However, the dystrophin-deficient *mdx* mouse shows no clinical signs of cardiac dysfunction. Our previous studies by MR tagging revealed a significant reduction of left ventricular torsion in old *mdx* mice despite preservation of global cardiac function [1]. However, the temporal evolution of regional contractile responses to defects in the DGC is still unknown. Accordingly, the objective of the present study was to characterize the very early manifestations of ventricular dysfunction using MR tagging as a sensitive method for improving therapeutic decision-making and follow-up. Surprisingly, we observed an early paradoxical increase in regional function followed later by decreased function, suggesting novel mechanisms for disease expression in this model of human muscular dystrophy.

Methods

MR imaging: *mdx* mice of two months (young, n=6), ten months (adult, n=6) and age matched C57/BL6 mice (n=7 for young group and n=5 for adult group) were scanned on a Varian 4.7T scanner with a 2.5 cm surface RF coil. Tagged images of five short-axis slices were acquired from apex to base with 1 mm slice thickness. The SPAMM1331 tagging sequence was applied immediately after the ECG trigger, followed by gradient-echo sequence with the following imaging parameters: TR, R-R interval; TE, 3 ms; field of view, 4 cm \times 4 cm; matrix size, 128 \times 256; tag resolution, 0.5 mm. Fifteen frames were acquired per cardiac cycle resulting in effective TR of 110-140ms. Two sets of tagged images were acquired with tags in perpendicular directions, yielding a tagging grid pattern when the two data sets were combined.

Histology: The hearts were fixed in 10% formalin and sliced at 1mm thickness from apex to base along the LV long-axis. The tissue sections were stained with Masson's trichrome for identification of myocardial scars. Each short-axis slice was scored according to the presence of scar tissue.

Data analysis: Images were analyzed with MATLAB-based software (CVMRI) developed in our laboratory. Epicardial and endocardial borders were traced interactively using B-spline interpolation. Intersecting tag points were tracked semi-automatically with a HARP-based approach [2]. Subsequently, LV twist, torsion and strains were calculated by 2D homogenous strain analysis.

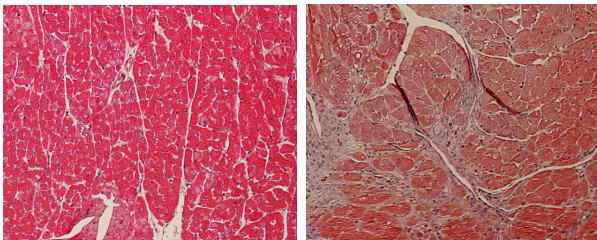


Figure 1. Masson's trichrome stained heart slices from a young *mdx* mouse (left) and an adult *mdx* mouse (right). Scar tissues appear in light blue.

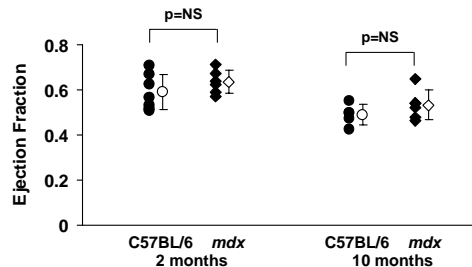


Figure 2. Scattered plot of ejection fraction of *mdx* and control mice in the two age groups.

Results

No scars were present in the young *mdx* mice. In the adult group, interstitial fibrotic patches or extensive transmural lesions were present in all the *mdx* mice (Figure 1). Despite the development of scar tissue, ejection fraction was similar between *mdx* and C57/BL6 mice in the adult group ($53.5 \pm 6.5\%$ vs. $48.9 \pm 4.7\%$, $p=NS$), as well as in the young group ($63.6 \pm 5.2\%$ vs. $58.9 \pm 7.9\%$, $p=NS$). The heart rate was also similar in *mdx* and control groups during MR scan (466 ± 50

BPM vs. 492 ± 34 BPM, $p=NS$ in the adult mice and 436 ± 63 BPM vs. 400 ± 66 BPM, $p=NS$ in the young mice).

The adult *mdx* mice exhibited significantly altered regional function that comprised decreased ventricular twist and circumferential strain (Figure 3A-B). As a result, ventricular torsion was also decreased from $2.74 \pm 0.52^\circ/\text{mm}$ in C57/BL6 to $1.87 \pm 0.41^\circ/\text{mm}$ in *mdx* mice ($p < 0.01$). Surprisingly, the young *mdx* mice exhibited enhanced ventricular twist and circumferential strain (Figure 3C-D). Accordingly, maximal torsion in the young *mdx* mice was also increased from $2.99 \pm 0.29^\circ/\text{mm}$ in C57/BL6 to $3.80 \pm 0.50^\circ/\text{mm}$ ($p < 0.01$).

Conclusion

Our results indicate that defective DGC causes a complex response in regional ventricular contraction during the disease progression, despite similarities in clinical indices of global cardiac function. The early increase in regional function may represent a compensatory mechanism that preserves ventricular function, but ultimately ventricular twist and strain decrease in the later stages in association with fibrosis and other manifestations of functional compromise. Although the source of this intriguing early augmentation in ventricular function remains to be defined, it is clear that the progression of disease does not follow a simple inexorable downhill course, suggesting that early therapeutic intervention might be beneficial when contractility and microanatomy are still well preserved.

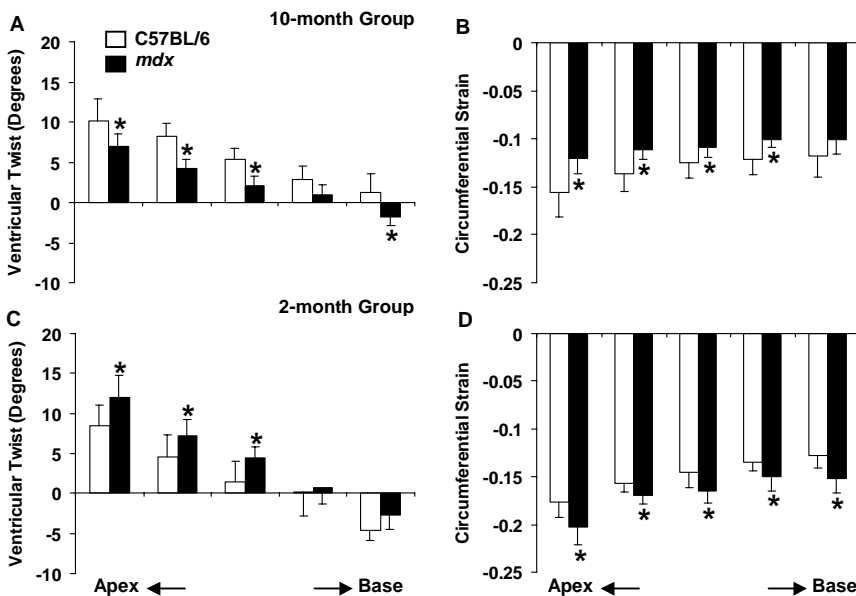


Figure 3. Ventricular twist (left column) and strain (right column) were reduced in the adult *mdx* mice (top row) and enhanced in the young *mdx* mice (bottom row). * $p < 0.05$

References: 1. Yu X. et al, Pro. Intl. Soc. Mag. Reson. Med. 2002.
2. Liu W. et al, Mag. Reson Med. 2004 (in press).